N O T I C E

THIS DOCUMENT HAS BEEN REPRODUCED FROM MICROFICHE. ALTHOUGH IT IS RECOGNIZED THAT CERTAIN PORTIONS ARE ILLEGIBLE, IT IS BEING RELEASED IN THE INTEREST OF MAKING AVAILABLE AS MUCH INFORMATION AS POSSIBLE

NASA

Technical Memorandum 80728

THE CONTRIBUTION OF THE DIFFUSE LIGHT COMPONENT TO THE TOPOGRAPHIC EFFECT ON REMOTELY SENSED DATA

Chris Justice
Brent Holben

June 1980

National Aeronautics and Space Administration

Goddard Space Flight Center
Greenbelt, Maryland 20771

THE CONTRIBUTION OF THE DIFFUSE LIGHT COMPONENT TO THE TOPOGRAPHIC EFFECT ON REMOTELY SENSED DATA

Chris Justice*

Brent Holben

June 1980

Code 923

NASA/GODDARD SPACE FLIGHT CENTER
Greenbelt, Maryland

*Chris Justice is currently an N.R.C. Resident Research Associate at the Earth Resources Branch, GSFC

CONTENTS

TABLES

TABLES (Continued)

ILLUSTRATIONS

ILLUSTRATIONS (Continued)

THE CONTRIBUTION OF THE DIFFUSE LIGHT COMPONENT TO THE TOPOGRAPHIC EFFECT ON REMOTELY SENSED DATA

Chris Justice
Brent Holben

ABSTRACT

The topographic effect is measured by the difference between the global radiance from inclined surfaces as a function of their orientation relative to the sensor position and light source. The shortwave radiant energy incident on a surface is composed of direct sunlight, scattered skylight and light reflected from surrounding terrain. The latter two components are commonly known as the diffuse component. The objective of this study was to examine the contribution of the diffuse light component to the topographic effect and to assess the significance of this diffuse component with respect to two direct radiance models, to spectral band ratioing and to simulated Landsat data.

Diffuse and global spectral radiances were measured for a series of slopes and aspects of a uniform sand surface in the red and photographic infrared parts of the spectrum, using a nadir pointing two-channel handheld radiometer. The diffuse light was found to produce a topographic effect which varied from the topographic effect for direct light. The topographic effect caused by diffuse light was found to increase slightly with solar elevation and wavelength for the channels examined. The correlations between data derived from two simple direct radiance simulation models and the field data were not significantly affected when the diffuse component was removed from the radiances. Diffuse radiances contributed largely to the variation in ratioed data. Subtraction of the diffuse radiance prior to ratioing resulted in a 50 percent average decrease in the standard deviation of the ratioed data.

In an extreme case of radiances from a 60 percent reflective surface, assuming no atmospheric path radiance, the diffuse light topographic effect contributed a maximum range of 3 pixel values in simulated Landsat data from all aspects with slopes up to 30 degrees. Such a variation is sufficiently small compared with other variations which are likely to occur in the data, to indicate that the diffuse component does not warrant modeling prior to cover classification analysis.

THE CONTRIBUTION OF THE DIFFUSE LIGHT COMPONENT TO THE TOPOGRAPHIC EFFECT ON REMOTELY SENSED DATA

1. INTRODUCTION

The shortwave radiant energy incident on a horizontal portion of the earth's surface is composed of direct sunlight, scattered skylight and light reflected from surrounding terrain. The latter two components are in common usage termed the diffuse component (Lui and Jordan, 1960; Stanhill 1966; Kondratyev, 1977). It is important to note that certain studies have used the term diffuse light to refer strictly to unpolarized light (Shurcliff, 1962). Throughout this study the common usage was adopted.

In modeling the sensor response from inclined surfaces, Holben and Justice (1979), Justice and Holben (1979), and Holben and Justice (1980) showed that there was a need to examine the contribution of the diffuse light radiance to the topographic effect. The topographic effect is defined here as the variation in global radiance from inclined surfaces as a function of their orientation relative to the sensor position and light sources. The term "topographic effect" is used because in the context of satellite remotely sensed data e.g., Landsat data, the light source and sensor geometry are essentially constant for a specific data set and the principal variation is in the surface geometry, i.e. topography. The degree of topographic effect can be measured by comparing the radiance from a horizontal surface to the radiance from a sloping surface of the same cover type. The objective of this paper was to quantify the contribution of the diffuse light component to the topographic effect through field measurement and to assess the significance of the diffuse light contribution both for two selected theoretical models and simulated Landsat data.

2. BACKGROUND

The irradiance received at a surface is the sum of the direct and diffuse components and is often termed the global irradiance. The diffuse skylight component impinging a surface is caused by the atmospheric Rayleigh and Mie scattering of the solar beam and varies in proportion to the direct

component as a function of wavelength, optical path length, composition of the atmosphere (Bullrich 1964, and Fraser 1975) and the orientation of the surface. Measurements of the intensity of diffuse radiation incident on a horizontal plane at the Earth's surface and the proportional relationship to the global flux have been presented both for clear skies (Iqbal 1979a and b) and cloudy conditions (Stanhill 1965). Measurement of the diffuse skylight is usually taken by obscurring the solar disc, although the effectiveness of this method is questioned by Heywood (1966). Measurements of the spectral distribution of both direct and diffuse components at varying times of year are presented by Boer (1977). Hourly, daily, and monthly totals of diffuse radiation calculated from surface measurements were described by Lui and Jordan (1960), Norris (1966) and Goldberg et al (1979). Diffuse and direct irradiance measurement have also been made for sloping surfaces by using hemispherical pyronometers tilted at various angles and aspects (Kondratyev and Manolova, 1960; Heywood, 1965; Temps and Coulson 1977; Klucher 1979). By definition, the diffuse skylight incident on a surface is multidirectional. The path length of atmospheric scatterers such as aerosols and air molecules changes with viewing direction and therefore the spectral distribution of skylight intensity would not be expected to be equal around the celestial hemisphere. This anisotropic distribution is important when considering the proportion of the diffuse component relative to the global irradiance impinging inclined surfaces.

The general distribution of the intensity of sky radiation has been presented by Bullrich (1964), Bullrich et al. (1968), Coulson (1971) and Temps and Coulson (1977) and shows an anisotropic distribution around the celestial hemisphere with a maximum around the solar aureole, caused by strong forward scattering and a minimum, normal to the solar beam in the principal plane. There is also a marked increase in brightness towards the horizon, due to limb brightening of the Earth. Temps and Coulson (1977) observed that for a 34° solar elevation that the intensity of skylight was 40 percent greater at the horizon that at the zenith.

Fedorova (1965) (referred to in Kondratyev 1977) showed that 80 percent of the total scattered flux incident on a horizontal surface will come from the circumsolar half of a clear sky. The

intensity of diffuse light reaches a peak between .4 and .5μm due to molecular Rayleigh scattering (Gates 1965, Dave et al. 1975) and the ratio of the irradiances of direct sunlight and global flux decrease with decreasing wavelength (Dave et al. 1975). The diffuse component of irradiance incident on a horizontal surface is greater than the direct component for wavelengths shorter than .375μm. The intensity and distribution of skylight around the celestial hemisphere is shown to vary both with solar elevation and wavelength (Voltz and Bullrich, 1961, Dave 1978, Bullrich et al. 1978).

Bullrich et al. (1968) show that the skylight minimum becomes angularly more distant from the sun with increasing solar elevation and wavelength. They reported that the skylight radiance differential between the solar zenith and the horizon increases with wavelength.

The relative proportion of diffuse to global irradiances increases directly with solar zenith angle (Frazer 1975), this increase being a maximum at large incidence angles (Coulson 1971). Temps and Coulson (1977) showed that under midlatitude, contenental summer, clear sky conditions, the skylight contributed 16 percent to the total flux on a horizontal surface, for a solar elevation of 37 degrees. Heywood (1966) states that the diffuse component on a clear sky midsummer day will rise from 16 percent of the total radiation at noon to 25 percent at 5 hours before or after noon. Dave et al. (1975) stated that the diffuse component on a horizontal surface is about one seventh of the direct component for the sun overhead but 1.2 times as much as the direct component for a solar zenith angle of 80°, under average midlatitude summer conditions.

Most studies of diffuse radiation are undertaken under clear sky conditions with no apparent visible haze. A change in aerosol content, water vapor and/or cloud cover will however cause a change in spectral intensity and spectral distribution of the skylight and a change in the relative proportions of direct and diffuse light. Detailed discussions of the intensity distribution of the skylight under different atmospheric conditions are given by Coulson (1971), Dave (1978) and Dave (1979).

The component of the diffuse light scattered from adjacent terrain contributes to the global flux incident on a surface but has received little attention in the literature due to the complexity of isolating this component for measurement. Light reflected from adjacent surfaces either onto the

measured surface, or into the sensor field of view will be dependent on a number of factors, such as directional reflectance characteristics, albedo and orientation of the adjacent surfaces. Heywood (1966) stated that terrain reflection and reradiation is negligible on surfaces of less than 60° slope, but can attain about 8 percent of the global radiation on a vertical surface in the summer.

Boer (1977) gave a general estimate of the contribution to the total sunlight by reflectance from adjacent surfaces of between 4 and 7 percent for surfaces normal to the solar beam, assuming a 20 percent surface albedo. Kondratyev (1977) stated that for steep slopes with high albedo values, the reflected radiation from surrounding terrain may constitute a considerable proportion of the global flux and that this proportion will be highest at low solar elevations for slopes facing away from the sun. In an example for a surface with a 20 percent albedo and in an extreme case (i.e., low solar elevation for slopes away from the sun), he reports that the terrain reflectance can constitute 69 percent of the global flux for a 90° slope and 9.8 percent for a 30° slope.

Modeling the radiation incident on surfaces has been undertaken for a number of applications. Recent developments in modeling the radiation from surfaces have been made for remote sensing applications (e.g., Oliver and Smith, 1974, Marks and Dozier, 1979, Kimes and Kirchner 1980), whereas previous insolation modeling had predominantly meteorological and solar energy applications. Several of the early models assumed an isotropic distribution for diffuse light under clear sky conditions. Lui and Jordan (1963) developed an insolation model to predict the global radiation on inclined surfaces assuming an isotropic diffuse sky distribution. Holben (1975) developed a direct and isotropic sky diffuse insolation model which incorporated first order effects due to slope orientation and shading from adjacent topography. However, several studies have shown the adverse effects of applying the isotropic diffuse sky assumption (e.g., Temps and Coulson 1977; Klucher 1979; Dave 1979). Kondratyev (1977) shows convincingly that the isotropic assumption is accurate for slopes facing perpendicular to the principal plane and for slopes of less than 45°.

The general anisotropic "all-sky" model presented by Klucher (1979) provides a good model for the solar radiation on tilted surfaces. The model was developed from horizontal surface measure-

ments and was shown to have a systematic error of less than 2.5mw/cm^2. This model showed improvements over the models presented by Lui and Jordon (1961) and Temps and Coulson (1977). Inclusion of the scattered terrain radiance in insolation models on inclined surfaces has been undertaken by Kondratyev (1977) Dozier (1978) and Kimes and Kirchner (1980) but these models are substantially more complex. Dozier (1978) developed a comprehensive solar radiation model for snow surfaces in mountainous terrain and in a sample of the model output of a typical mountainous situation, showed the following results: for the ultraviolet and visible spectrum 75 percent of the incoming radiation was direct, 15 percent diffuse and 10 percent from terrain reflectance; for the infrared 91 percent was direct, 2 percent diffuse, and 7 percent terrain reflectance. Kimes and Kirchner (1980) demonstrated that exclusion of adjacent terrain reflectance when modeling Lambertian target reflectance under extreme conditions, i.e. adjacent slopes of 30°; sun angle corrected albedo of 5 percent; infrared wavelength, could lead to a 9 percent error. The error term was considerably less for slopes under 30°.

For remote sensing studies and in particular examination of the topographic effect we are concerned with radiance emanating from the surface and not solely the insolation or irradiance impinging the surface and thus we need to consider the reflection of both the direct and diffuse components. The radiance measured from a surface is a function of the reflectance properties of the surface, the atmosphere between the ground and the sensor, the sensor geometry, and the incident radiation. Examination of the diffuse radiance component in the context of remote sensing will help us to model the topographic effect more accurately and to assess its significance in models applied to satellite remotely sensed data. For non-Lambertian surfaces, the radiances will be determined by the directional scattering properties of the surface, the intensity and direction of radiation sources, and the exitance angle and therefore radiance modeling will undoubtedly be more complex than for Lambertian surfaces.

3. GROUND DATA COLLECTION

The approach adopted for quantifying the diffuse light component to the topographic effect was to measure diffuse and global radiances from surfaces tilted at a range of slopes and aspects. Radiances were measured consecutively from a non-Lambertian coarse sand surface and a $BaSO_4$ reference surface. The $BaSO_4$ surface approximates a Lambertian surface and has a reflectance of approximately 98%, for the wavelengths and view angles examined in this study. At steeper view angles a $BaSO_4$ surface approximates a Lambertian surface far less (Schutt 1976, Hsia and Richmond 1976). The Lambertian reference plate provides a measure of the irradiance on the surface and can be used to calculate the surface reflectances. The reflectances calculated for different light source and sensor geometries are termed reflectance factors (Judd, 1967). The term bidirectional reflectance factor is more commonly used (Kriebel, 1977, Nicodemus et al., 1977) and for a specified wavelength gives a measure of the amount of light reflected into the sensor, relative to the total amount of light impinging the surface. More detailed discussions of the bidirectional reflectance factors from natural surfaces are given by Coulson et al., (1965), Coulson (1966), Kriebel (1976, 1977, 1978), and Robinson and Biehl (1979).

Radiance measurements were obtained for both surfaces, inclined at all combinations of slope angles, ranging from 0-60 degrees in 10° increments and aspects for the 16 compass points, in 22.5° increments. The surface aspect was measured in degrees clockwise from the sun's azimuth. This angle is termed the "azpect" of the surface (Holben and Justice, 1979). Red and photographic infrared radiance data pairs were collected in data subsets called "azpect strings," that is slopes between 0 - 60° in 10° increments for each azpect. The measurements, in π radiances, were taken using a two-channel nadir pointing handheld radiometer, similar to that described by Pearson et al. (1979), filtered for the red (0.63 - 0.69 μm) and photographic infrared (0.76 - 0.90 μm) bands. These channels are equivalent to the proposed Thematic Mapper bands 3 and 4 of Landsat D (Tucker et al., 1980). Although π radiances were measured using the handheld radiometer, the term radiance is used to describe these measurements throughout the text.

The surfaces surrounding the target were painted flat black to minimize terrain scattering. Global and diffuse radiances were measured for both surfaces at each slope/azpect combination. The diffuse observations were obtained by shielding the solar disc with a small opaque panel. Three data sets were taken under clear sky conditions for solar elevations of 23°, 29°, and 39°, which correspond to the Landsat sensing time for midlatitude solar elevations occuring during late fall, winter and early spring, or for high latitude solar elevations occuring during late spring, summer and early fall respectively. Each data set was collected in less than 45 minutes and each azpect string in less than 3 minutes. The measurement apparatus was reoriented to the sun's azimuth after collection of radiance measurements for each azpect string subset, to reduce errors due to the apparent movement of the sun.

4. ANALYSIS

The analysis of the data is presented in four subsections. The first section (4.1) describes the general characteristics of the diffuse light topographic effect. Section 4.2 shows how the diffuse light topographic effect changes with solar elevation and wavelength. Section 4.3 assesses the significance of the diffuse component with respect to two direct radiance models and to spectral band ratioing. The final section (4.4) demonstrates by a simulation study, the contribution of the diffuse light topographic effect to Landsat MSS sensor response.

4.1 General Characteristics of the Diffuse Light Topographic Effect.

A topographic effect is observable when a change in radiance occurs due to a change in surface orientation. This topographic effect can be quantified by subtracting the radiance measured from a horizontal surface from the radiance measured from an inclined surface. Variations in diffuse radiance from the $BaSO_4$ surface were observed between slope angles and orientations (Figure 1) and therefore by definition a topographic effect was apparent due to the diffuse component. The greatest radiance range occurred in the principal plane of the sun and the smallest range for slopes perpendicular to the principal plane. An increase in radiance with slope occurred for all azpects. This pat-

tern strongly resembles the anisotropic distribution of diffuse light around the celestial hemisphere, described in Section 2. The variation in the diffuse radiance values is directly related to variations in the sky brightness. The maximum sky radiance in the solar half of the celestial hemisphere explains the greater radiance values associated with a given slope angle, for those azpects close to solar azimuth. The strong positive relationship between slope and radiance can be explained by the limb brightening of the Earth and a possible contribution from terrain reflectance at the higher slope angles. The close correspondence between the anisotropic sky distribution and radiance would be expected from a Lambertian surface, as the radiances are directly related to the intensity of the impinging radiation and are independent of the view angle.

All natural surfaces are non-Lambertian and to some degree have preferred orientations of scattering, i.e. angular anisotropy of reflection (Kriebel 1976). The radiances from non-Lambertian surfaces are therefore dependent on view angle. The degree of departure from Lambertianess determines the magnitude with which radiances will be affected by view angle. The diffuse radiance values for the coarse sand surface in the photographic infrared (0.76 - 0.90 μm) (Figure 2), reveal a similar pattern to that displayed by the Lambertian radiances (Figure 1), namely a marked increase in radiance with slope. Examination of the radiances for the same slope angle with different azpects (i.e., the concentric circles in Figure 2) reveals little variation, indicating that the scattering from this non-Lambertian surface is not particularly orientation dependent. This is most likely due to the random distribution of the sand grains and their individual reflecting surfaces. The similarity between the coarse sand and $BaSO_4$ surfaces indicates that the sand surface has no extreme preferred direction(s) of scattering. This is confirmed by examination of the direct and diffuse light reflectances for each slope and azpect combination (Figures 3a and b). The reflectance as shown in Figures 3a and b is the ratio of the radiance from the non-Lambertian surface (coarse sand) to the radiance from the Lambertian reference surface ($BaSO_4$) for a given slope and azpect. The relatively constant reflectance values for the same slope angle at different azpects (Figures 3a and b) show the lack of orientation dependence of scattering from the sand surface. The difference between the reflectances in

Figure 3b indicates that the isotropic assumption for the diffuse light will not accurately model the radiance. Although in this case the natural surface examined did not show any marked directional scattering, it can be hypothesized that the variations in sky brightness combined with the reflectance properties of the surface will make diffuse radiances from natural surfaces complex to model.

4.2 Variations in the Diffuse Light Topographic Effect with Wavelength and Solar Elevation.

The diffuse light topographic effect for the $BaSO_4$ surface in the red part of the spectrum (0.63 - 0.69 μm) illustrates the same general pattern in the radiances (Figure 4) as for the infrared (Figure 1) portion of the spectrum. Both the diffuse radiance values and the range for each azpect were lower for the red than the photographic infrared, the wider photographic infrared bandwidth examined in this study, resulted in higher overall radiance values. The decrease in the radiance values for 0-20° slopes facing away from the solar azimuth, is caused by the dominance of the skylight minimum radiance in the exposed portion of the celestial hemisphere, relative to the contribution from the horizon and surrounding surface reflectance.

Variations in the $BaSO_4$ diffuse light radiances were present for all data sets collected. Examples for 23° and 39° solar elevations in the red and infrared wavelengths are presented in Figures 5a, b, c, and d. In general, higher solar elevation data sets had higher diffuse radiances and slightly greater ranges in the radiances associated with an azpect string, particularly in the photographic infrared (Table 1). Table 1 shows a slight increase in the diffuse light topographic effect. The increase in the radiance with solar elevation is due to the smaller angle of incidence made with the surface and the resulting increase in the global flux through a decrease in atmospheric path length. It should be noted that although the diffuse radiances increase with solar elevation, the proportion of the diffuse component relative to the direct decreases.

Calculated differences in the topographic effect for three solar elevation data sets, as measured by the range in radiances associated with each azpect, showed that the greatest variation in the radiance ranges between data sets, occurred for those slopes facing into solar azimuth (Table 1). The

topographic effect was essentially the same for those azpects facing away from solar azimuth and varied less for the red channel.

4.3 The Relative Proportion of the Diffuse Light Component to the Global Radiance Received by the Sensor.

In the previous two sections, the analysis dealt with the magnitude and variability of the diffuse light topographic effect but to understand the contribution of this component to the topographic effect, it is necessary to consider the magnitude of the diffuse radiance relative to the global radiance. The amount of diffuse light received by the sensor relative to the global radiance from the $BaSO_4$ surface was calculated as a percentage and is plotted by slope and azpect for two solar elevations, 39° and 23° (Figures 6a and 6b respectively). Little change was observed in the proportion of diffuse light reaching the surface for those azpects facing into solar azimuth, although a marked increase in the proportion of the diffuse component occurred with slope, for those azpects perpendicular to and away from solar azimuth (Figure 6a and 6b). A marked increase occurs as incidence angles of 90° are approached (i.e., at grazing angles). For azpects facing into sun there is a general decrease in percentage diffuse light with increasing slope. This is counteracted by terrain reflectance at high slopes, i.e. greater than 40°. The same general pattern can be seen for the two solar elevations (Figures 6a and 6b), but it should be noted that more slopes are in shadow for the 23° data set. The data for lower sun elevations showed a smaller percent diffuse component for slopes facing into sun and a larger percent for those facing away from solar azimuth. The proportion of diffuse light for the horizontal surface is similar for both data sets (i.e., c. 13 percent). The variation in radiances with azpect for the horizontal surface is caused by slight changes in solar elevation during the measurement procedure. The topographic effect caused by the diffuse component was more pronounced at low sun angles, than at high sun angles (Figures 6a and 6b). Although the absolute diffuse radiances are smaller at low sun angles, the proportion of the total incoming diffuse radiation is generally higher. The contribution of the diffuse component to the topographic effect varies considerably with azpect (Figures 6a and 6b). Although the diffuse radiances vary relatively little compared to the direct

radiances, the relative proportions of each component vary considerably, indicating that an isotropic assumption for diffuse light would fit the field data with differing degrees of success, depending on slope and azpect configuration and solar elevation.

4.4 Assessing the Significance of the Diffuse Component for Two Direct Radiance Models and Spectral Band Ratioing.

The significance of the diffuse component can only be assessed with reference to a given application of the radiance data. In this study, we are concerned with the significance of the diffuse component in modeling radiance data to eliminate the topographic effect. One way to evaluate this significance is to examine the effect of the diffuse component on two previously used direct radiance models (Justice and Holben, 1979), by correlating theoretical radiances from the radiance models to the measured global radiances and the calculated direct radiances. A second assessment of the significance of diffuse radiation is undertaken by examining the effect of the diffuse component on spectral band ratioing.

The significance of the diffuse component on the correlation between the field measured data and simulated data derived from sunlight models proposed by Justice and Holben (1979) was assessed. Data derived from the simple Lambertian model (Cos i) was correlated with the global radiance for the $BaSO_4$ surface, for a sun elevation of 39°. The direct radiance was calculated by subtracting the diffuse radiance from the global radiance. A small improvement in the coefficients of determination (r^2) of up to 6 percent was obtained for the radiances with the diffuse component subtracted. The improvement was particularly marked for those azpects perpendicular to solar azimuth. Correlation coefficients for the data derived using a non-Lambertian model, $Cos^k i \cdot Cos^{k-1} e$ (Justice and Holben 1979, Smith et al. 1980), were calculated with the global and direct radiance. An average improvement of 26 percent in the coefficient of determination for the radiances with the diffuse component subtracted over the coefficients for the global radiance was observed for those azpects perpendicular to the solar azimuth, but a minimal improvement (i.e. less than 1 percent) was observed for all other azpects.

The results from the correlation analysis indicated that subtraction of the diffuse component leads to very little improvement in the simulation of the radiance by the two direct models examined, with the notable exception of those azpects perpendicular to the solar azimuth. In this case, the correlation analysis provides only a coarse measure of the degree of association between the direct models and the radiance data. For an explanation of correlation results, it is necessary to examine detailed plots of the diffuse and direct data (Figure 7). For the 23° and 39° solar elevation data sets, it can be seen that both the diffuse and direct radiances increase with slope for those azpects facing solar azimuth. For slopes facing away from solar azimuth the direct radiances decrease while the diffuse radiances increase. The negative relationship between the diffuse and direct radiances and the high proportion of the diffuse radiance relative to the direct radiance at 90° azpect, accounts for the marked increase in the coefficient of determination for the direct radiance models when the diffuse component is extracted from the global radiance.

The second assessment of the significance of the diffuse component is with reference to band ratioing to remove the topographic effect. Band ratioing has been shown to provide a means of reducing the topographic effect on remotely sensed data (Vincent, 1973). As the diffuse component of the radiance has been shown to vary with wavelength, band ratioing of two spectral channels (i.e., Channel i/Channel j) will not lead to complete elimination of the topographic induced variations (Holben and Justice 1980).

To assess the effect of the diffuse light component on band ratioing of the two channels, the ratios were calculated for both the global and direct radiances for all slopes and azpects (Figure 8). Subtraction of the diffuse component from the radiance data, led to a 50 percent average decrease in the standard deviation in the ratioed values for all azpect classes. The degree of reduction was greatest, approximately 75 percent, for azpects perpendicular to the principal plane and least, approximately 20 percent, for azpect classes parallel to the principal plane.

The large decrease in the standard deviations of the direct light ratio values from the global radiance ratios, is due to diffuse skylight, which cannot be removed by simple band ratioing. The results from this analysis show that the diffuse component contributes significantly to the variation in spectral band ratioing and prevents ratioing from completely removing the topographic effect in the field data.

4.5 Assessing the Diffuse Light Contribution to Simulated Landsat MSS Radiances.

The field measurements examined in this study represent an ideal controlled data set which may help to predict the topographic effect on other sensors of multispectral data. Landsat MSS data are perhaps the most widely used type of remotely sensed multispectral data in earth resources analysis and have been shown to exhibit marked topographic effects in the areas of rugged terrain (Holben and Justice, 1979). In an effort to assess the importance of the diffuse component on Landsat radiance data, the field measured radiances collected in this study were converted to Landsat 3 (MSS 5 and 7) pixel value equivalents. The simulated pixel values were obtained by converting the hand-held radiometer radiances to radiance values that would be received by the Landsat sensor, given specified atmospheric conditions and then quantising the radiances according to the linear response of the Landsat 3 analogue-to-digital converter. The method used for this simulation study is detailed in the appendix and was used in a Landsat simulation study by Tucker (1979). The object of this simulation study was to demonstrate the range of pixel values (i.e., Landsat quantization levels), that could be expected from the diffuse component and thereby assess the importance to cover classification and modeling the topographic effect on Landsat data. Radiances derived from both the $BaSO_4$ and the coarse sand surface were used for this study. The $BaSO_4$ surface had c. 98 percent reflectance which was far higher than the reflectance from most natural surfaces and in certain cases led to saturation of the simulated satellite sensors. The coarse sand surface had approximately 60 percent reflectance. These two surfaces represented some of the highest radiances from natural surfaces that would be obtained by the satellite for the solar elevations in question and would in turn result in the greatest possible topographic effect. Similarily the range of slopes examined

0 -60°, represented a far greater range than is commonly found even in areas of rugged terrain and therefore exaggerated the degree of topographic effect that could be expected. To provide a more realistic representation of the diffuse light topographic effect on Landsat data, the range of simulated pixel values was calculated for 0 - 30° slopes for each azpect, as well as for the complete azpect string (Table 2). The greatest range in simulated pixel values for the sand surface for the 0 - 60° slopes was 9, for the 0° azpect in MSS 7, whereas the maximum range for the 0 - 30° slopes was 3 pixel values.

A maximum range of 3 pixel values for the diffuse light from a 60 percent reflecting surface for all azpects at slopes of 0 - 30° leads to the question of whether consideration of the diffuse component should be included in analysis of Landsat data. The reflectances associated with most natural surfaces fall well below 60 percent and as such the diffuse topographic effect would be even smaller. Given the range of pixel values associated with any cover type it is unlikely that the diffuse topographic effect would be significant for cover type discrimination. However, where adjacent surface reflectances and slopes are high the diffuse component may need to be considered.

5. DISCUSSION OF RESULTS AND CONCLUSIONS

The diffuse light contribution to the topographic effect was described as a function of solar elevation, atmospheric conditions, surface geometry, surface reflectance properties; and surrounding terrain reflectance. The results presented in this study, although specific for the particular conditions and surfaces examined, detail a number of general trends and implications common for a range of solar elevations that can be extrapolated to other studies. Additionally this study evaluated the importance of the diffuse light component for three normalization techniques.

Quantification of the diffuse radiances showed a marked topographic effect, the greatest variation being in the principal plane. Radiances from the $BaSO_4$ and sand surface were found to increase with slope and for the range of surface orientations examined, were strongly influenced

by the anisotropic skylight distribution. Radiances from high angle slopes were slightly increased by light reflected from surrounding terrain. The sand surface used in this study was found to exhibit no preferred orientation of scattering. The diffuse radiances exhibited the same pattern in both the channels examined, although the diffuse radiances were larger and the topographic effect was higher for the photographic infrared channel than for the red channel. The higher radiances were due to the wider bandwidth of the infrared channel. Although the diffuse radiances varied relatively little compared to the direct radiances, the proportion, of the diffuse light relative to the direct light varied considerably, particularly for slopes facing away from solar azimuth.

Both the diffuse radiances and the diffuse topographic effect were found to increase with solar elevation. The diffuse light component under clear sky conditions for the horizontal surface ranged from between 10 and 14 percent of the global radiance solar for elevations for 23 to 39°. However, radiances recorded at low solar elevations were found to have a smaller percentage diffuse component for slopes into solar azimuth and greater percentage diffuse component for slopes away from solar azimuth than at higher solar elevations.

The contribution of the diffuse light topographic effect to the overall topographic effect within global radiances, varies with azpect; the diffuse radiances generally increasing with slope for azpects facing into sun and decreasing with slope for azpects perpendicular and away from sun. These results indicate than an isotropic sky assumption cannot be used to adequately describe the diffuse component.

Assessment of the significance of the diffuse component was undertaken first by examining the effect on two direct radiance models. Only slight improvements were found in the correlation between the radiance and the theoretical data derived using the Lambertian Model, whereas an average improvement of 26 percent in the correlation coefficient was calculated for data derived using the non-Lambertian model when the diffuse component was subtracted.

The significance of the diffuse component to band ratioing was also assessed. Subtraction of the diffuse component led to a 50 percent average decrease in the standard deviation of the ratios associated with the uniform surface, over the range of slopes and azpects examined. The greatest reduction in the standard devaitions was found for slopes perpendicular to solar azimuth.

The Landsat simulation study showed that for clear sky conditions over a range of solar elevations associated with typical mid-latitude Landsat passes, that the diffuse light radiances in cases of extreme reflectance and slope variation would constitute only a maximum 3 pixel variation in the Landsat measured global radiances. In this event, it is unlikely that such a maximum variation could be taken into consideration to improve cover classification accuracies, by reducing the diffuse light topographic effect. It should be understood that areas of shadow will have 100 percent diffuse radiance and the higher Landsat quantization values associated with these shadowed areas are essentially due to atmospheric path radiance. The effect of varying atmospheric path radiance between the target and sensor were not examined in this study.

One method used to eliminate the diffuse component and incoming path radiance effects from Landsat radiance data is dark object subtraction (Bentley et al., 1976). For this method the lowest radiance within the scene is subtracted from all the radiances prior to ratioing. This method assumes an isotropic sky distribution and a Lambertian surface and, depending on the range of diffuse radiance values in the scene, will lead to an over or underestimation of the radiances and subsequent distortion of the resulting ratios.

Diffuse light causes a topographic effect on remotely sensed data which will vary in significance with the application in question. The ground based study showed that the diffuse component caused a detectable variation in the ratioed spectral data which potentially could be modeled and hence the effect eliminated from the data. For Landsat studies a maximum possible variation of 3 pixel values for the conditions specified does not at present warrant further detailed modeling

and in most cases the variation due to the diffuse component will be substantially less.

ACKNOWLEDGEMENTS

The authors wish to thank John Townshend and Jim Tucker for their help with the collection and analysis of the data used in this study.

BIBLIOGRAPHY

Bentley, R. G., C. Bette, D. Salmon et al., 1976. A Landsat study of ephemeral and perennial rangeland vegetation and soils. Final Report. Bureau of Land Management. 234 pp.

Boer, K. W., 1977. The solar spectrum at typical clear weather days. Solar Energy 19 p. 525-538.

Bullrich, K. 1964. Scattered radiation in the atmosphere and the natural aerosol. Advances in Geophysics; Vol. 10 (H.E. Landsburg and J. Von Miegham, eds) p. 101, Academic Press.

Bullrich, K., W. Blattner, T. Conley et al., 1968. Research on atmospheric radiation transmission. Interim scientific report No. 6 (AFCRL No. 0186). Meteorology and Geophysics Institute, Gutenberg University, Mainz, Germany.

Coulson, K. L. 1966. Effects of reflection properties of natural surfaces in aerial reconnaissance. Applied Optics, Vol. 5 (6) p. 905-917.

Coulson, K. L. 1971. On the solar radiation field in a polluted atmosphere. J. Quart. Spectrosc. Radiat. Transfer, Vol II pp. 739-755.

Coulson, K. L., G. M. Bouricius and E. L. Gray. 1965. Optical reflection properties of natural surfaces. J. Geophys. Res., Vol. 70 (18) p. 4601-4611.

Dave, J. V. 1978. Extensive data sets of the diffuse radiation in realistic atmosphere models with aerosols and common absorbing gases. Solar Energy, Vol. 21 pp. 361-369.

Dave, J. V., 1979. Isotropic distribution approximation in solar energy estimations. Solar Energy, Vol. 22 p. 15-19.

Dave, J. V., P. Halpern and B. Braslau. 1975. Spectral distribution of the direct and diffuse solar energy received at sea-level of a model atmosphere. IBM Palo Alto Scientific Center technical report No. G320-3332. 20 pp.

Dozier, J. 1978. A solar radiation model for a snow surface in mountainous terrain Proc. Modeling of Snow Cover Runoff, U.S. ACRREL p. 144-153.

Fedorova, M. P., 1965. Scattered radiation fluxes from individual regions of the sky to inclined surfaces. Probl. Atm. Physc., Coll. Papers No. 3 pp. 129-137.

Fraser, R. S., 1975. Interaction Mechanisms Within the atmosphere. In. R. G. Reeves (ed) Manual of remote sensing. Vol. 1, Chapter 5 p. 181-229. Am. Soc. Photogramm.

Gates, D. M., 1971 Radiant energy, its receipt and disposal. Agricultural Meterology, Meterorological Monographs Vo. 6 No. 28 p. 1-24, Am Soc. Meteorol.

Goldberg, B., W. J., Klein, and R. D., McCartney, 1979. A comparison of some simple models to predict solar irradiance on a horizontal surface. Solar Energy 23(1) p. 81-83.

Heywood, H. 1966. The computation of solar radiation intensities. Part 2. Solar radiation on inclined surfaces. Solar Energy 10 (1).

Holben, B.N. 1975. The development and sensitivity analysis of a model for estimating insolation climate in mountainous topography. Masters Thesis,Colorado State University, Fort Collins, 159 pp.

Holben, B. N. and C. O. Justice 1979. Evaluation and modeling of the topographic effect on the spectral response from nadir pointing sensors. NASA/GSFC Tech. Mem. 80305, p. 20.

Holben, B. N. and C. O. Justice, 1980. An examination of spectral band ratioing to reduce the topographic effect on remotely sensed data. NASA/GSFC Tech. Mem. 80604, p. 28.

Hsia, J. and J. C. Richmond. 1976. A high resolution laser bidirectional reflectometer with results on several optical coatings. Journal of Research (National Bureau of Standards) Vol. 80A No. 2, 190-205.

Iqbal, M. 1979a. A study of Canadian diffuse and total solar radiation data I. Solar Energy 22(1), 81-86.

Iqbal, M. 1979b. A study of Canadian diffuse and total solar radiation data II. Solar Energy 22(1), 87-90.

Judd, D. B. 1967. Terms, definitions, and symbols in reflectometry. J. Opt. Soc. Am. 57(5), 445-452.

Justice, C. O. and B. N. Holben. 1979. Examination of Lambertian and non-Lambertian models for simulating the topographic effect on remotely sensed data. NASA/GSFC Tech. Mem. 80557 p. 20.

Kimes, D. and J. Kirchner. 1980. Modeling the effects of various radiant transfers in mountainous terrain on sensor response. E.R.B., NASA/GSFC Paper submitted ot IEEE Geoscience and Remote Sensing.

Klucher, T. M. 1979. Evaluation of models to predict insolation on tilted surfaces. Solar Energy 23. pp. 111-114.

Kondratyev, K. Va., 1977. Radiation regime on inclined surfaces. World Meteorological Organization, Tech. Note, 152.

Kondratyev, K. J. and M. P. Manolova. 1960. The radiation balance of slopes. Solar Energy, IV (1), 14-19.

Kriebel, K. T. 1976. On the variability of the reflected radiation field due to differing distributions of the irradiation. Rem. Sens. Env., 4, 257-264.

Kriebel, K. T., 1977. Reflection properties of vegetated surfaces: Tables of Measured Spectral Biconical reflectance factors. Wissenschaftliche Mitteilung Nr. 29. University of Munich Meteorological Institute, pp. 81.

Kriebel, K. T. 1978. Measured spectral bidirectional reflection properties of four vegetated surfaces. Applied Optics 17, (2), 253-259.

Lui, B. Y. H. and R. C. Jordan, 1960. The interrelationship and characteristic distribution of direct, diffuse and total solar radiation. Solar Energy IV, No. 3, 1-19.

Marks, D. and J. Dozier, 1979. A clear sky radiation model for remote alpine areas. Arch. Met. Geoph. Biokl., Ser. B.,27, 159-187.

Nicodemus, F. E., J. C. Richmond, et al., 1977. Geometrical considerations and nomenclature for reflectance. NBS Monograph 160, U. S. Rept. of Commerce. pp. 51.

Norris, D. J., 1965. Solar radiation on inclined surfaces. Solar Energy, 10(2), 72-76.

Oliver, R. E. and J. A. Smith 1974. A stochastic canopy model of diurnal reflectance. Final Report. U. S. Army Research Office, Durham, North Carolina, DAH CO4-74-60001, pp. 105.

Pearson, R. L., L. D. Miller and C. J. Tucker 1976. Handheld spectral radiometer to estimate gramineous biomass. Applied Optics, Vol. 15, 416-418.

Robinson, B. F. and Biehl L. L. 1979. Calibration procedures for measurement of reflectance factor in remote sensing field research. Proc. SPIE, Vol. 196, Measurements of Optical Radiation p. 16-26.

Schutt, J. B., 1976. Understanding bidirectional reflectance and transmission for space applications. Journal of Research (National Bureau of Standards) Vol. 80A No. 4, 597-603.

Shurcliff, W. A., 1962. Polarized light, production and use. Harvard Univ. Press, Cambridge, Mass.

Smith, J., Tseu Lie Lin and K. J. Ranson, 1980. The Lambertian assumption and Landsat data. Paper submitted to Photogramm. Eng. and Rem. Sensing.

Stanhill, G., 1965. Diffuse sky and cloud radiation in Israel. Solar Energy, Vol. 10(2), 96-101.

Temps, R.C., and K. L. Coulson, 1977. Solar radiation incident upon slopes of different orientations. Solar Energy 19, 179-184.

Tucker, C. J., 1979. Radiometric resolution for monitoring vegetation: How many bits are needed? NASA/GSFC Tech Mem. 80293, pp. 20.

Tucker, C. J., W. H. Jones, W. A. Kley, and G. J. Sundstrom 1980. A three band hand-held radiometer for field use. NASA/GSFC Tech. Mem. 80641, pp. 20.

Vincent, R. K., 1973. Spectral ratio imaging methods for geological remote sensing from aircraft and satellites. In Proc. Am. Soc. Photogramm. Management and Utilization of Remote Sensing Data Conf. Sioux Falls S.D., 377-397.

Volz, F. E., and K. Bullrich, 1961. Scattering function and polarization of skylight in the ultraviolet to the near-infrared region. Journal of Meteorology, 18, 306-318.

APPENDIX. CONVERSION OF RADIANCES TO LANDSAT QUANTIZATION LEVELS

The diffuse radiances measured by the hand-held radiometer were converted mathematically to radiances that would be received by the Landsat multispectral scanner (MSS) sensors. These radiances were then quantized according to the linear response of the Landsat 3 analog to digital converter.

The two spectral channels of the hand-held radiometer were filtered to represent the proposed Thematic Mapper (TM) bands 3 and 4 of Landsat D (0.63-0.69 μm and 0.76-0.90 μm). These two channels are sufficiently similar to the MSS channels 5 and 7 (0.6-0.7 μm and 0.8-1.1 μm) of Landsat 3, to enable the following simulations.

The Landsat 3 MSS sensors are calibrated in mw/cm^2 -sr. To convert the hand-held radiometer radiances from W/m^2 in the TM bandwidth to the MSS calibration, the radiances were divided by 10 (W/m^2 > mw/cm^2), divided by π to convert to a steradian measure and multiplied by the ratio of the appropriate MSS bandwidth to the TM bandwidth. This procedure assumes no atmospheric degradation or contribution to the observed signal. For this simulation study we chose the extreme example of the maximum MSS response to the diffuse radiance emanating from the surface, from a target of uniform cover and infinite extent.

Once the radiances were calculated, they were quantized from 0-127 levels (2^7 bite). Table A provides the maximum/minimum MSS radiances necessary to form the linear regression for quantizing the radiance data.

Table A. Minimum and maximum radiances (mw/cm^2 - sr) corresponding to quantization levels 0-127.

MSS Channel	Quantization Level 0	127
4	.04	2.50
5	.03	2.0
6	.03	1.65
7	.03	4.50

Source: Grelowsky, 1980, Personal Communication, NASA/GSFC.

Regression equations were calculated for each band and the slopes (m) and intercepts (b) are presented in Table B. The regression equation takes the form of:

Quantization Level = m x Radiance + b

Table B. The slopes and intercepts of the linear quantization regression presented for each MSS channel.

Band	Slope (m)	Intercept (b)
4	51.62623	-2.06505
5	64.47453	-1.93424
6	78.39448	-2.35183
7	28.43332	-0.85300

The calculated quantization level for each radiance was rounded to the nearest whole number which functionally corresponds to the MSS analog to digital converter on board Landsat 3.

Table 1. The diffuse light topographic effect for three solar elevations, showing the range in radiance (W/m^2-sr) associated with each azpect for the barium sulphate surface.

	23°		29°		39°	
	Red	Photo IR	Red	Photo IR	Red	Photo IR
Azpect 0	1.7	6.7	2.9	7.8	2.9	8.3
45	1.3	6.1	2.2	6.9	2.4	8.0
90	.9	6.2	.8	5.8	1.1	6.7
135	.8	6.5	.8	6.5	.7	6.5
180	.7	5.9	.7	6.4	.7	7.0
225	.9	6.3	1.0	6.8	.9	6.9
270	.8	4.9	1.9	6.1	1.4	7.4
315	1.3	5.1	2.2	7.1	2.5	8.1

Table 2. Simulated Landsat pixel ranges for diffuse light by azpect.

		MSS 5	MSS 7	MSS 5	MSS 7
Azpect (degrees)	Slope Range (degrees)	C. Sand		$BaSO_4$	
0	30	2	3	5	5
	60	5	9	10	15
45	30	2	2	4	4
	60	4	8	8	13
90	30	0	2	1	3
	60	2	8	2	11
135	30	0	1	0	2
	60	0	3	1	5
180	30	1	1	1	3
	60	1	1	1	3
225	30	0	1	0	3
	60	0	1	0	3
270	30	1	3	2	4
	60	2	8	3	12
315	30	2	2	5	5
	60	4	8	8	14

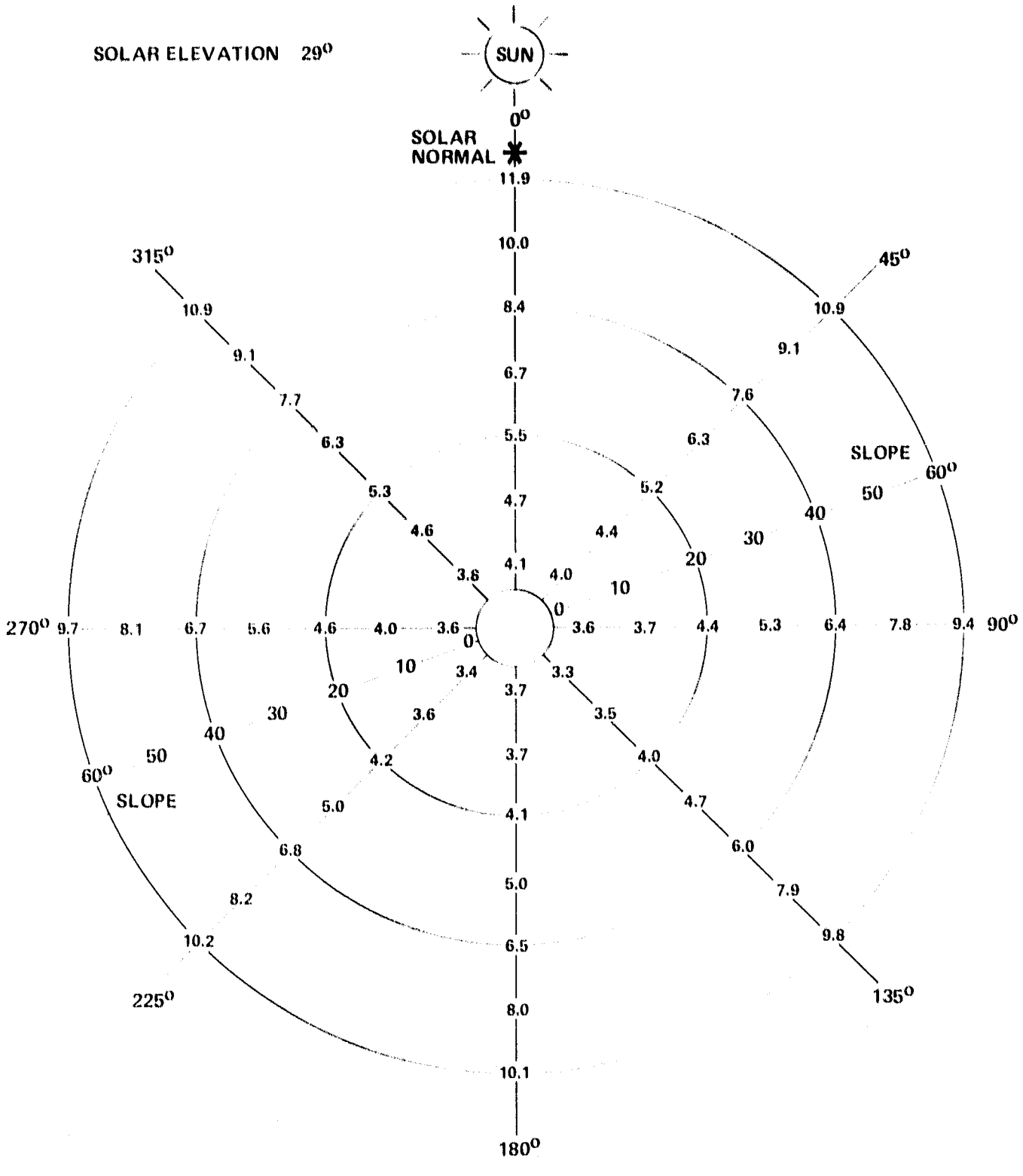

Figure 1. Diffuse Radiance (W/m^2 - sr) (.76 - .90 μm) Plotted By Slope and Azpect - Barium Sulphate Surface

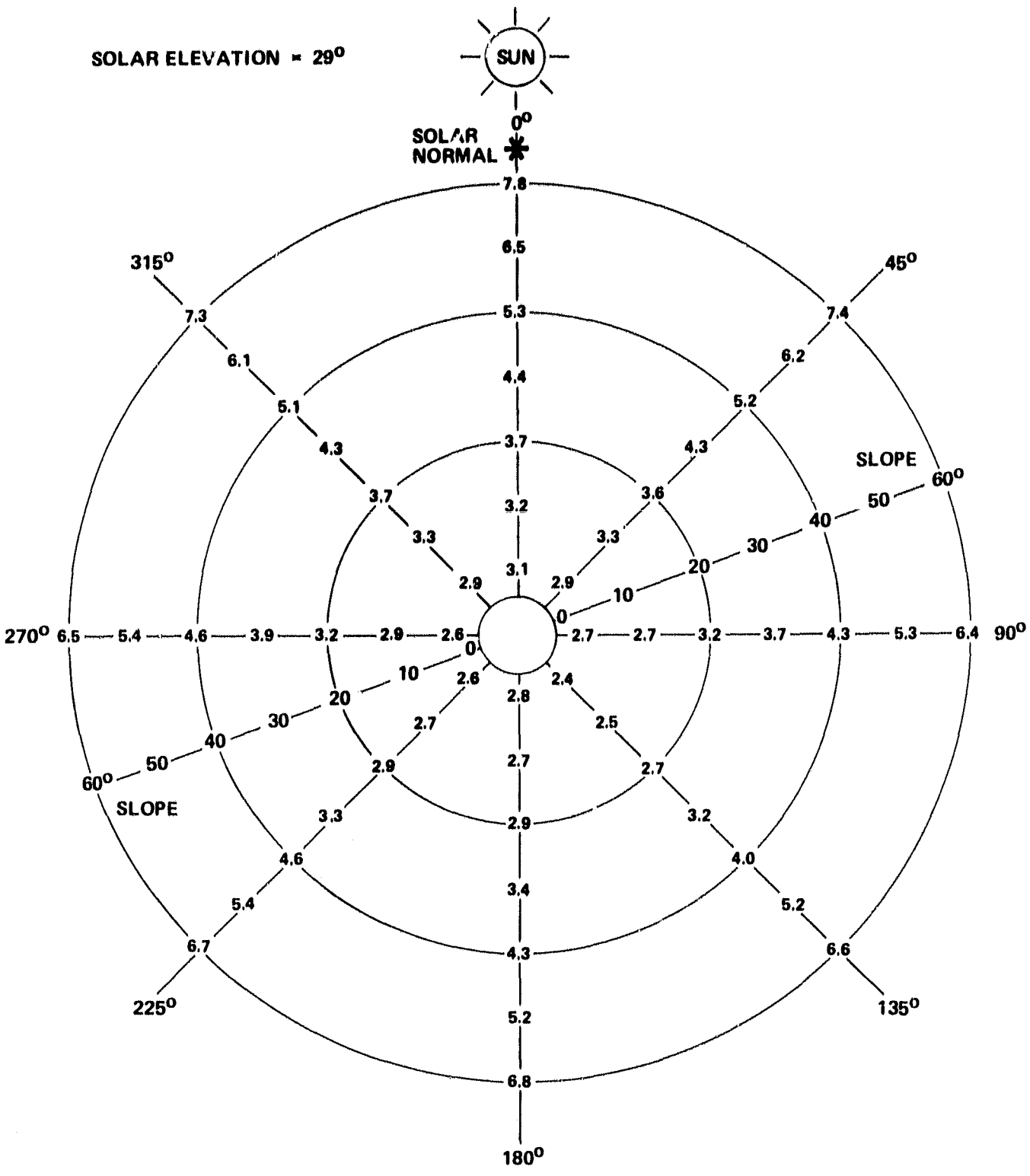

Figure 2. Diffuse Radiance (W/m^2 - sr) (.76 - .90 μm) Plotted By Slope and Azpect - Coarse Sand Surface

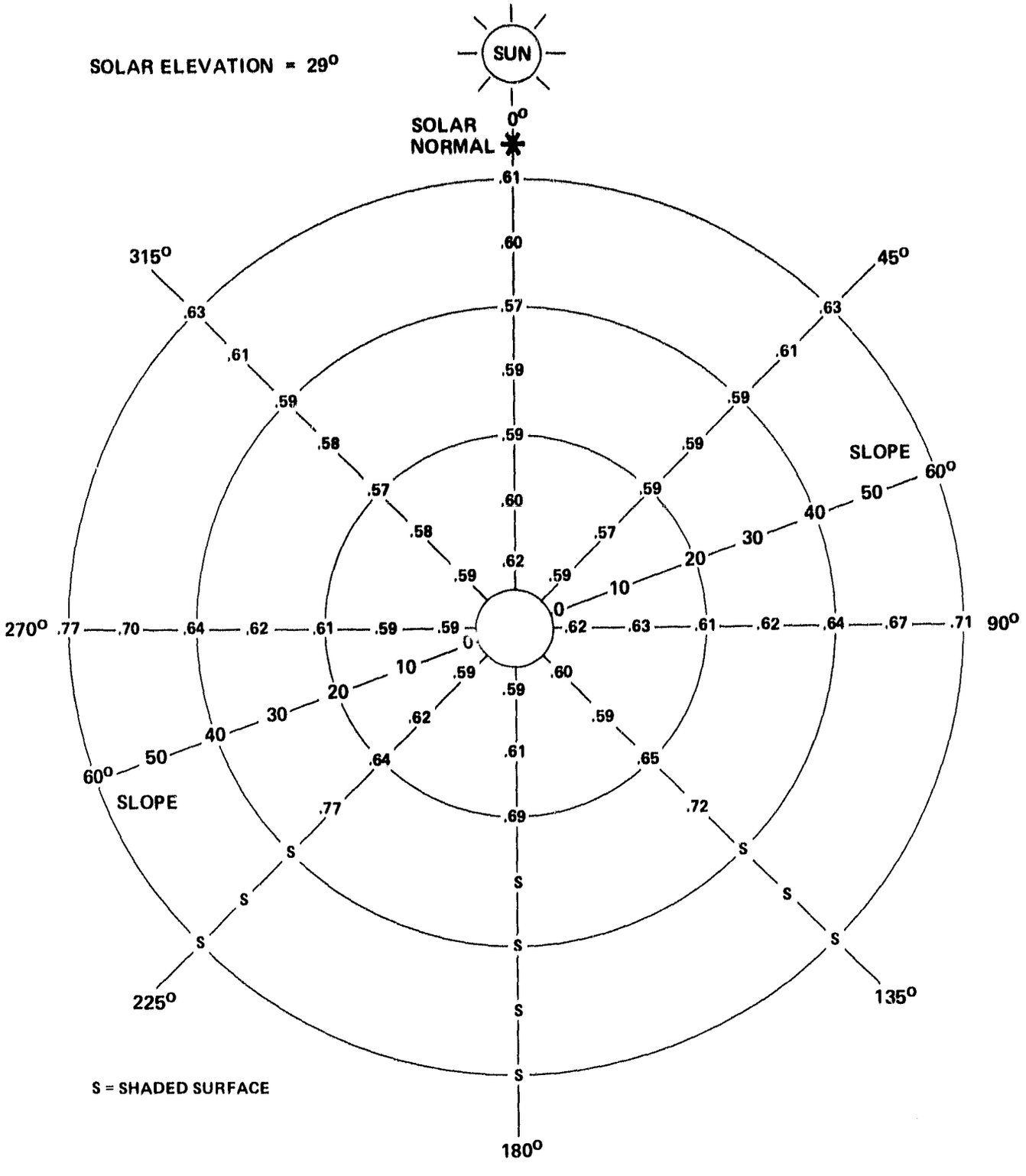

Figure 3a. Reflectance Values for Direct Light (.76 - .90 μm) Plotted by Slope and Azpect - Coarse Sand Surface

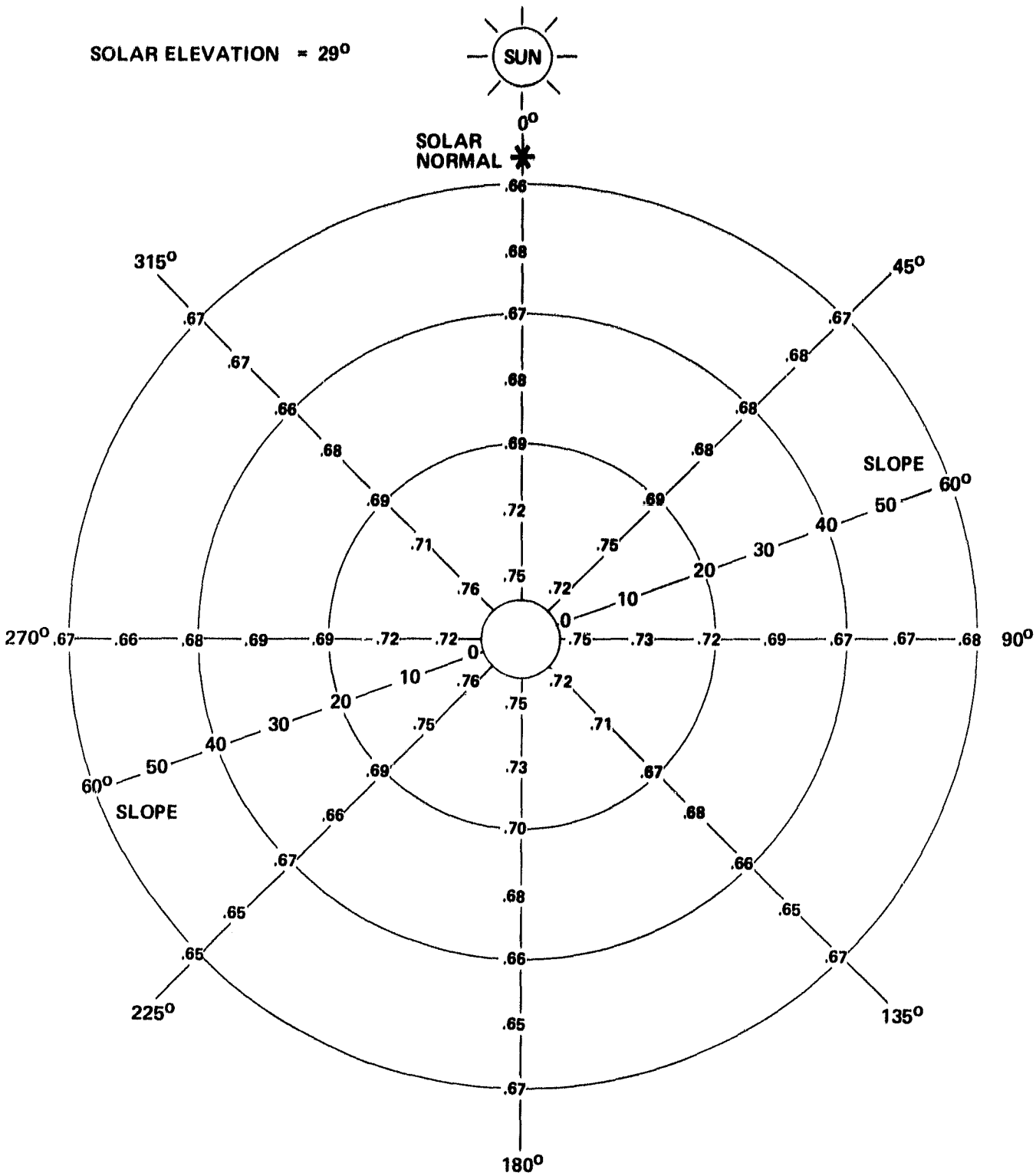

Figure 3b. Reflectance Values for Diffuse Light (.76 - .90 μm) Plotted by Slope and Azpect - Coarse Sand Surface

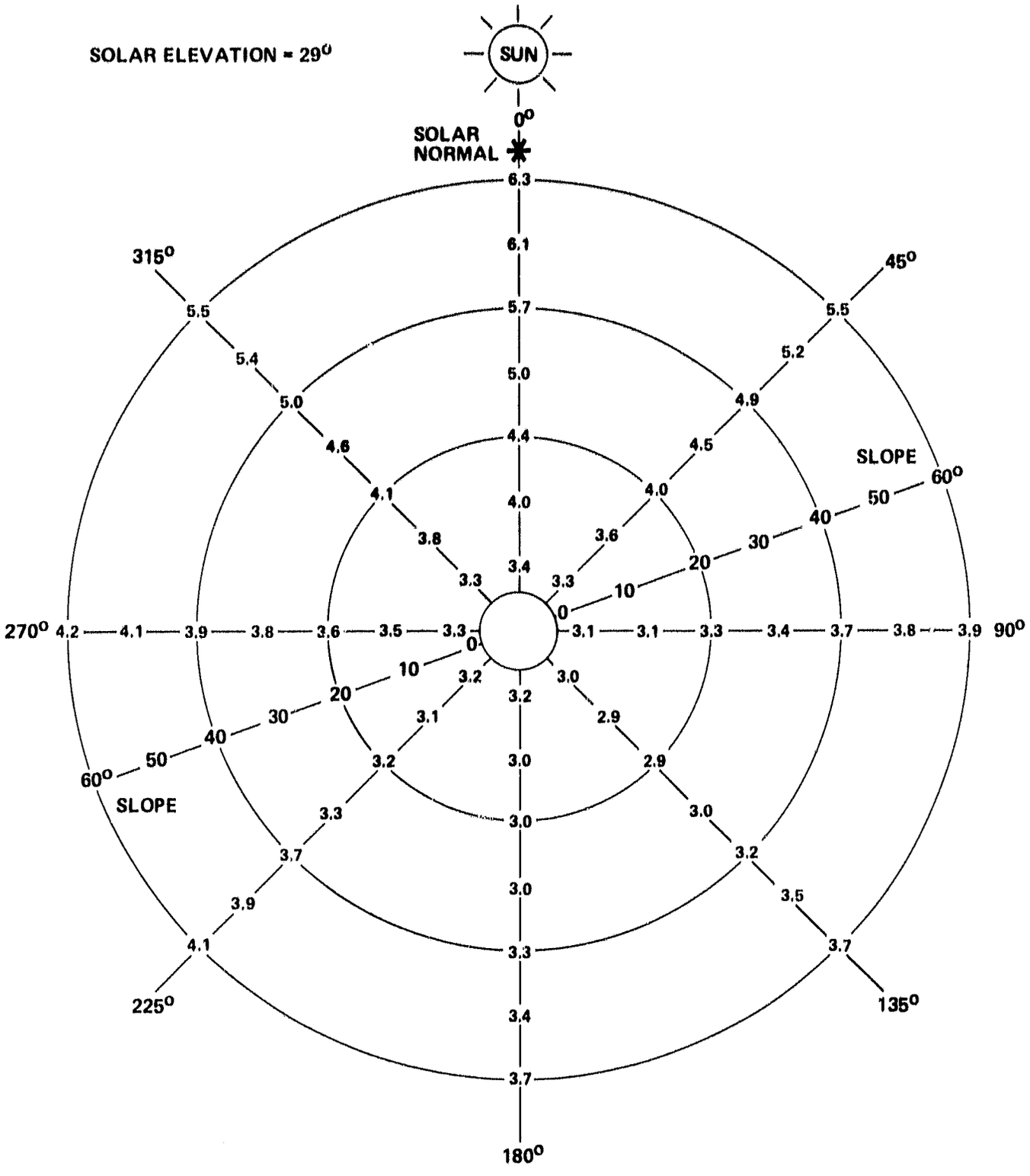

Figure 4. Diffuse Radiance (W/m^2 - sr) (.63 - .69 μm) Plotted by Slope and Azpect - Barium Sulphate Surface

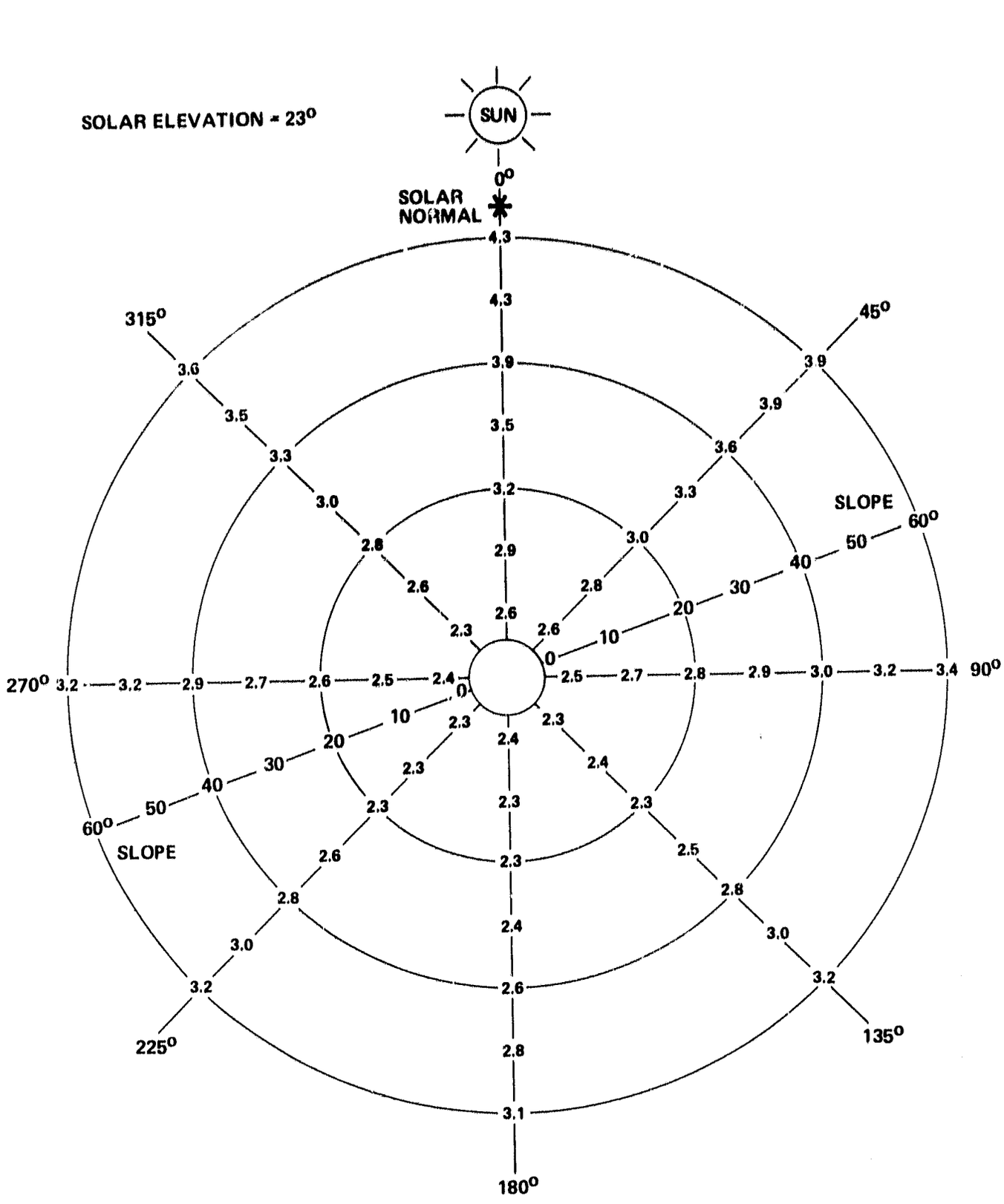

Figure 5a. Diffuse Radiance (W/m^2 - sr' ,63 - ,69 μm) Plotted by Slope and Azpect - Barium Sulphate Surface

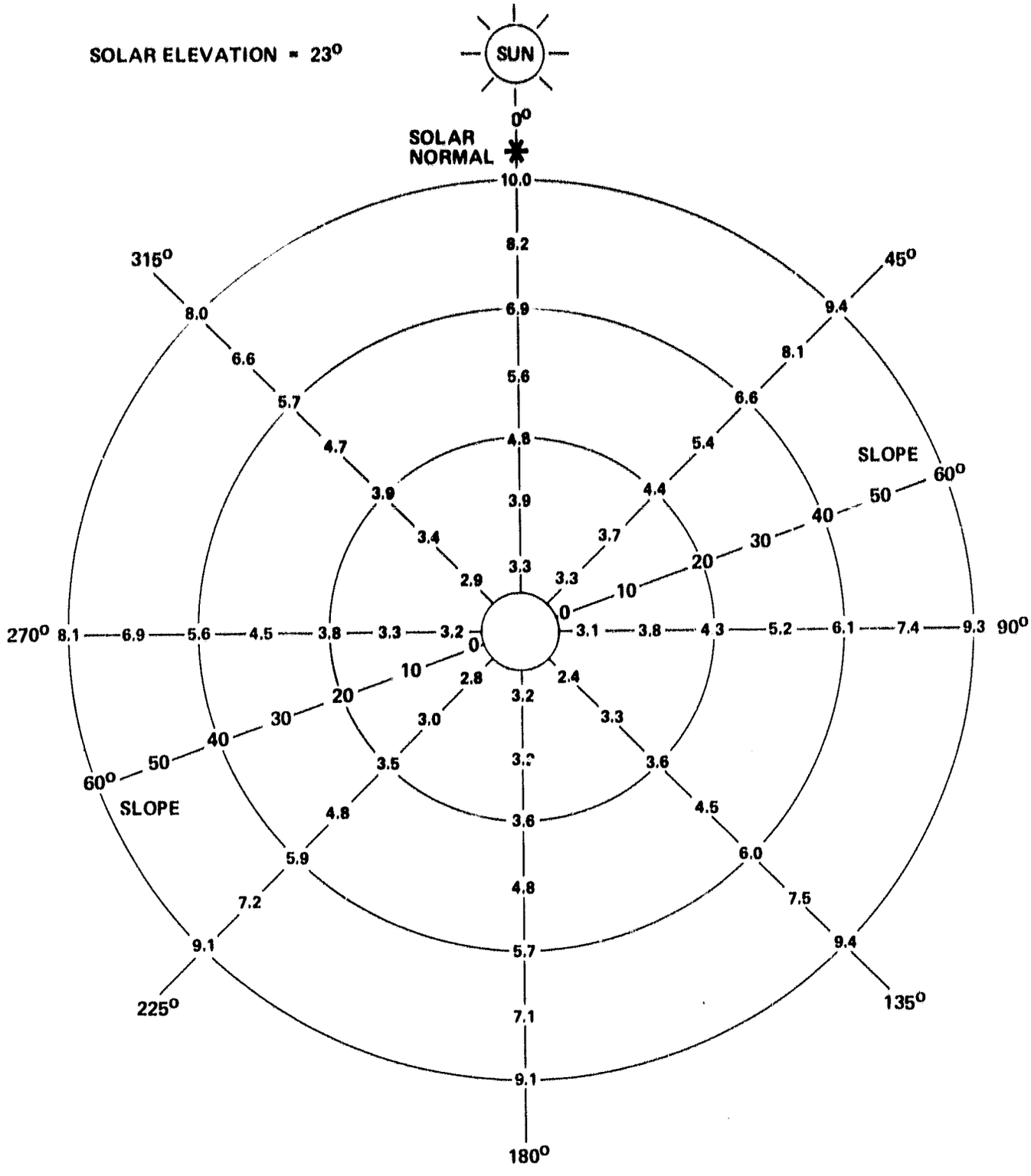

Figure 5b. Diffuse Radiance (W/m^2 - sr) (.76 - .90 μm) Plotted by Slope and Azpect - Barium Sulphate Surface

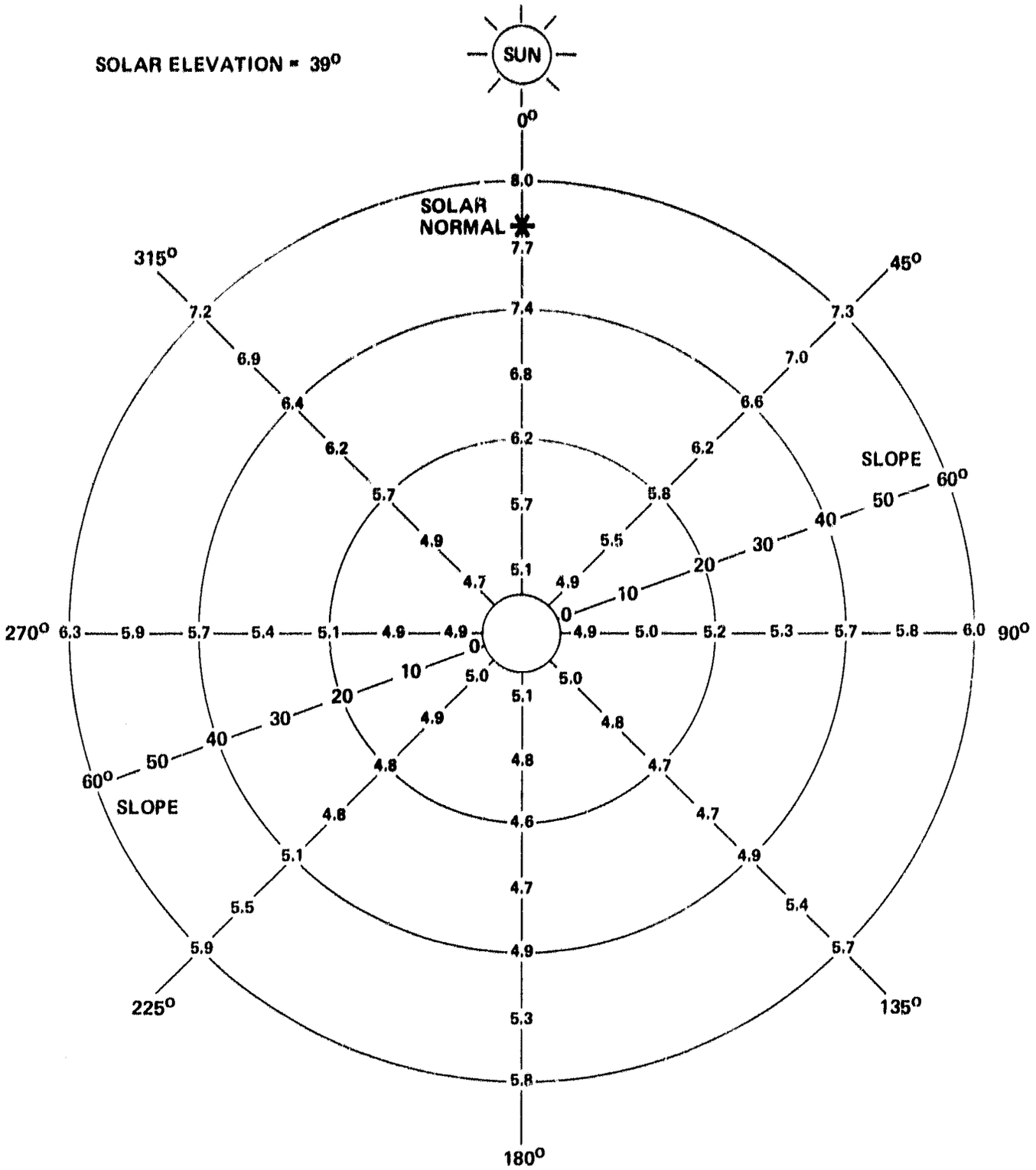

Figure 5c. Diffuse Radiance (W/m^2 - sr) (.63 - .69 μm) Plotted by Slope and Azpect - Barium Sulphate Surface

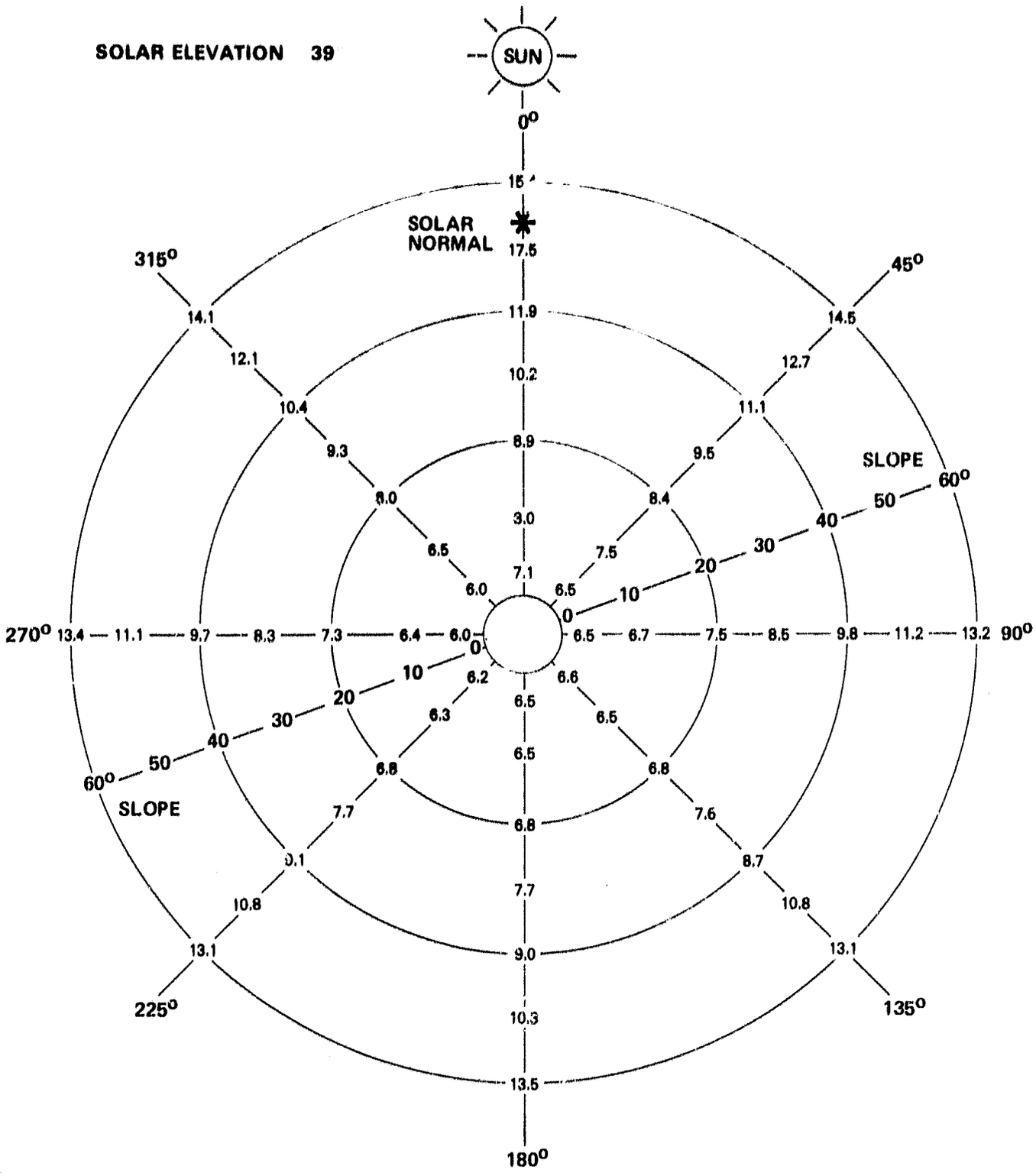

Figure 5d. Diffuse Radiance ($W/m^2 \cdot sr$) (.76 - .90 μm) Plotted by Slope and Azpect - Barium Salphate Surface

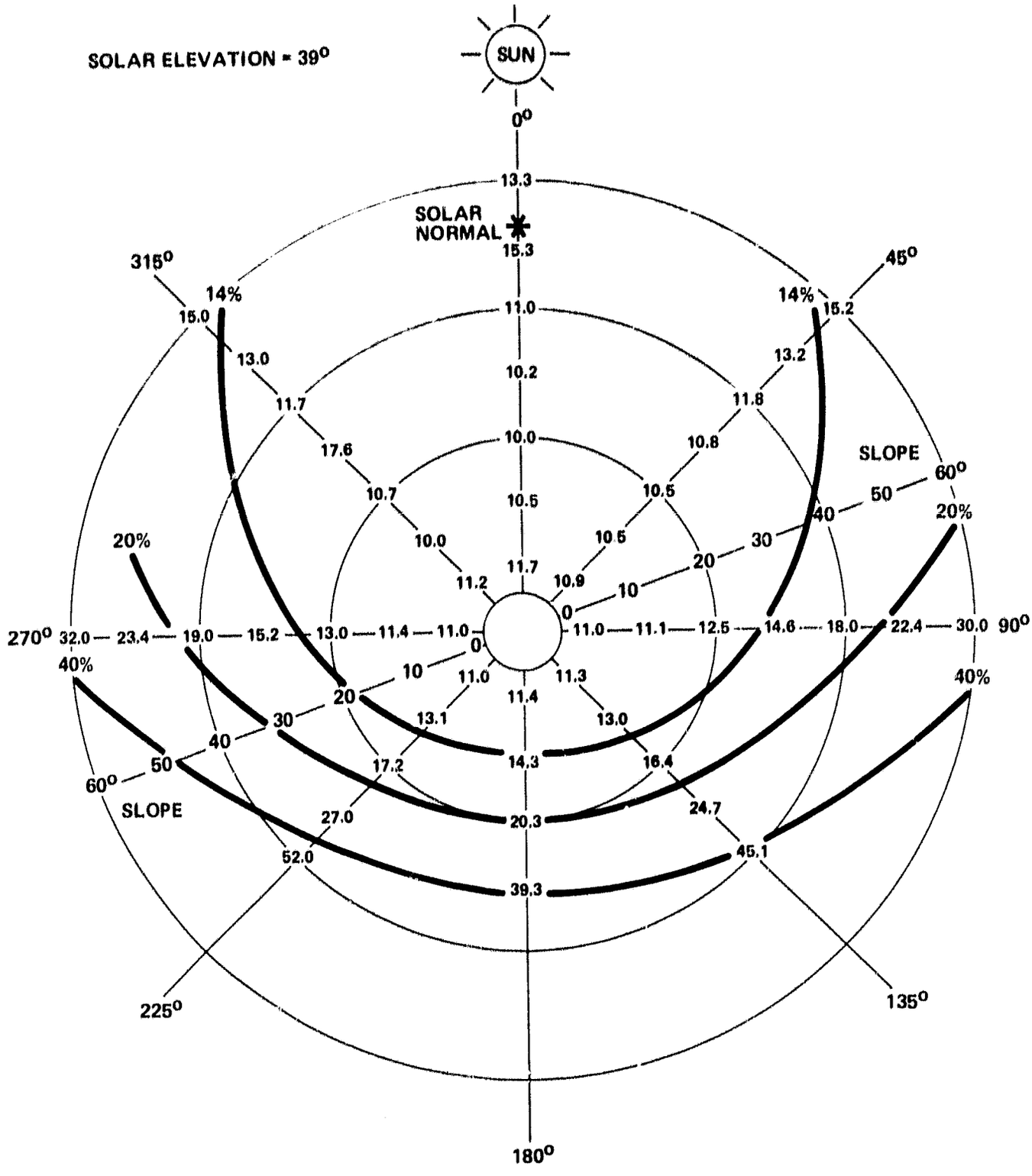

Figure 6a. Percentage Diffuse Sunlight (.63 - .69 μm) Plotted by Slope and Azpect - Barium Sulphate Surface

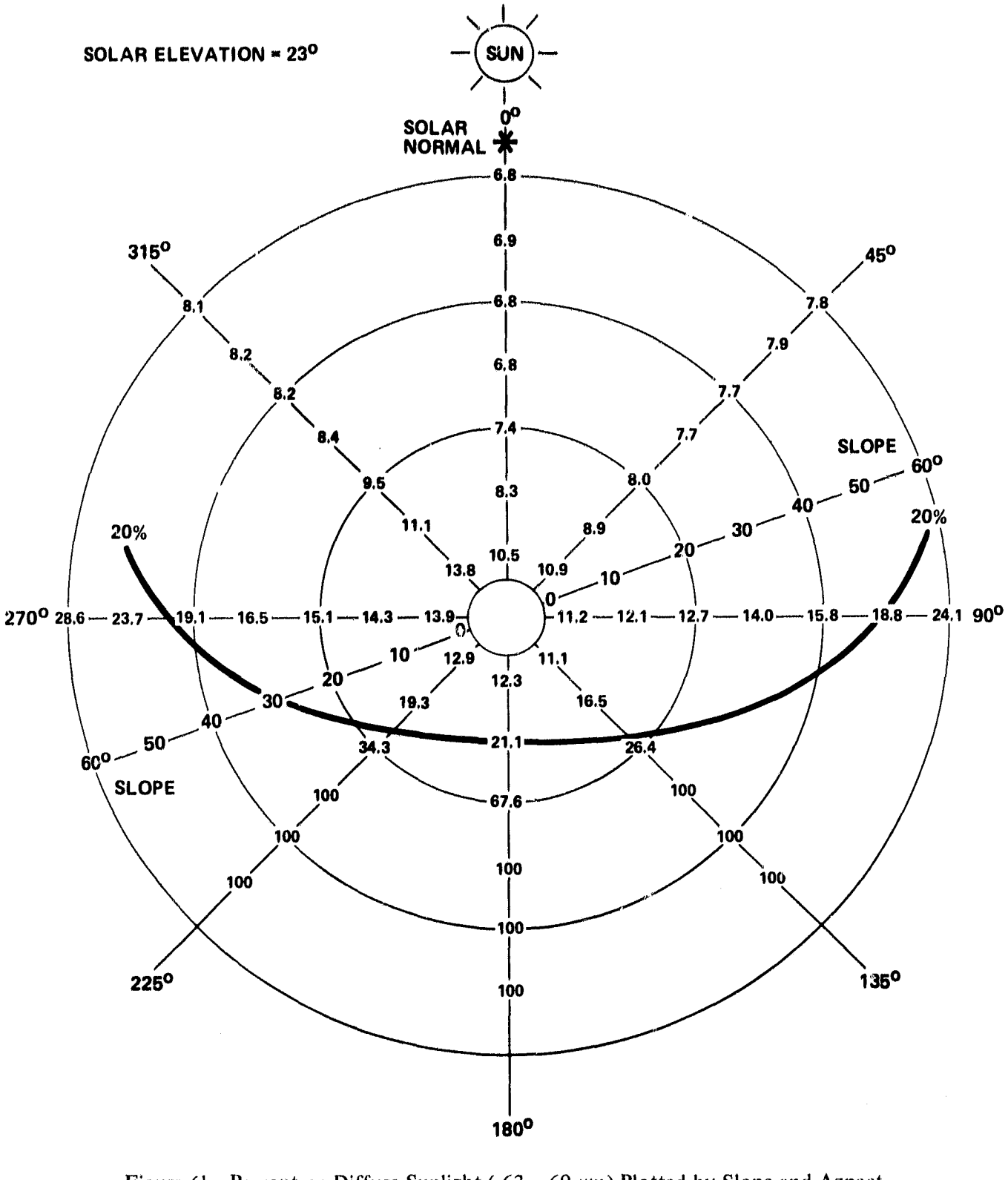

Figure 6b. Percentage Diffuse Sunlight (.63 - .69 μm) Plotted by Slope and Azpect - Barium Sulphate Surface

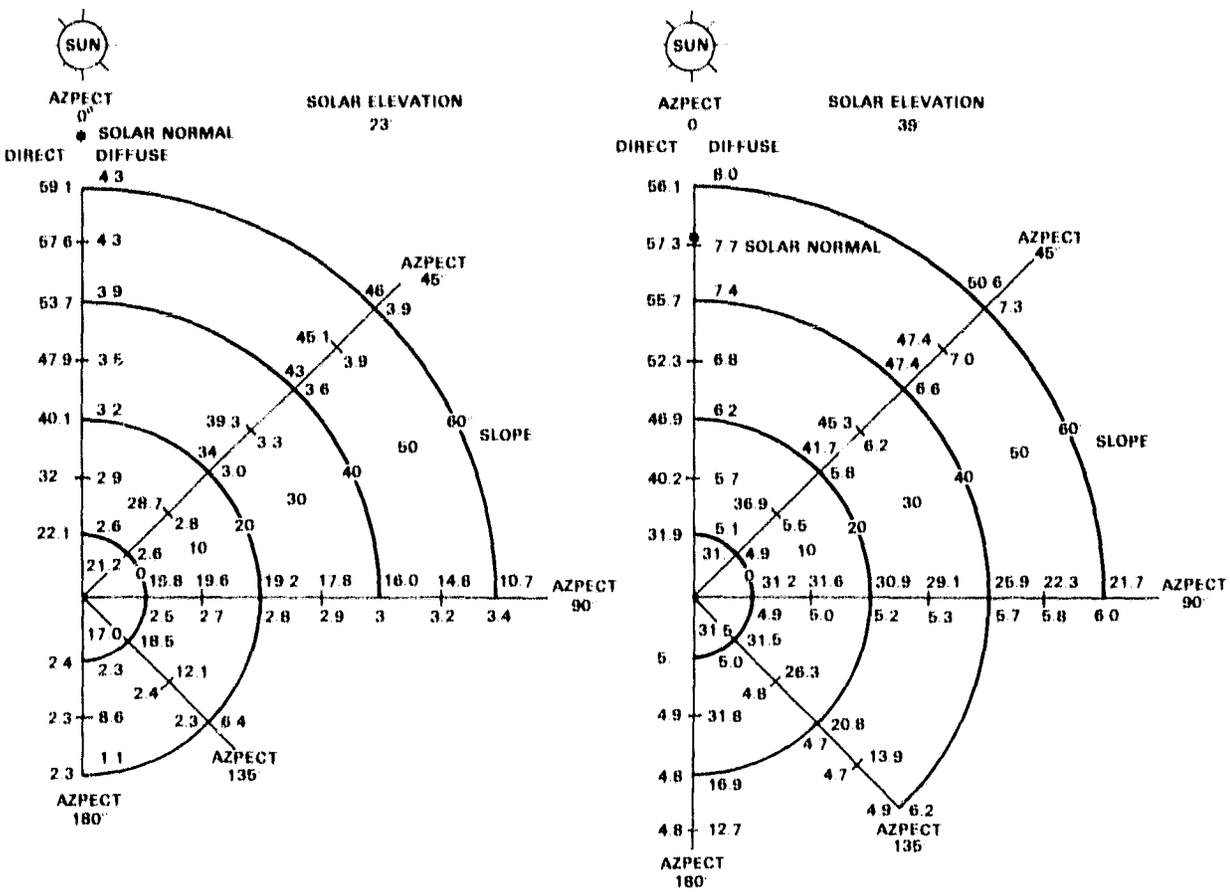

Figure 7. Direct and Diffuse Light (W/m^2-sr) (.63 - .69μm) Plotted by Slope and Azpect for Two Solar Elevations

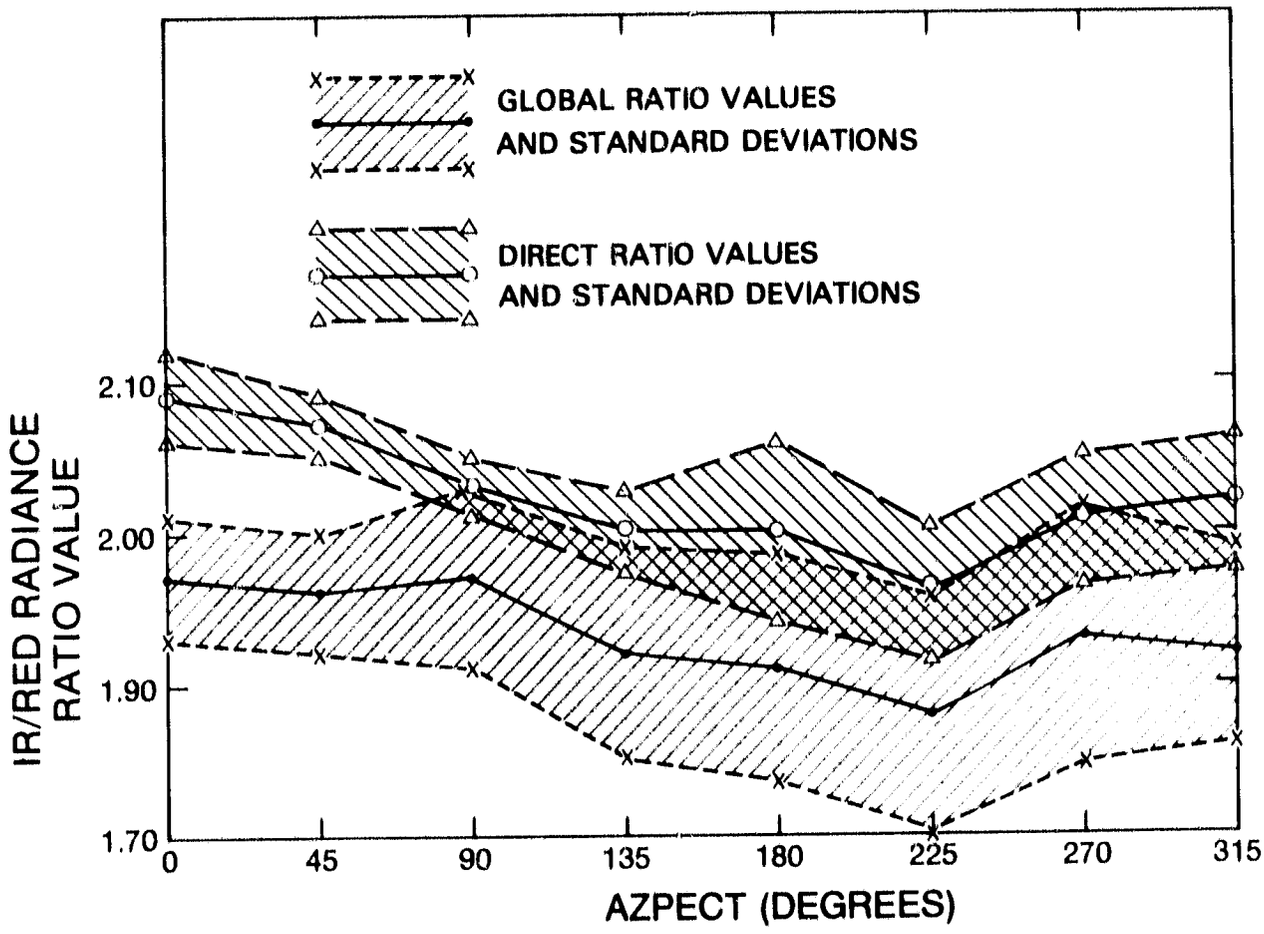

Figure 8. IR/RED Radiance Values and Standard Deviations Calculated from Global and Direct Radiances vs. Azpect